International Journal of Pharmaceutics: X 7 (2024) 100242

Contents lists available at ScienceDirect

International Journal of Pharmaceutics: X

journal homepage: www.sciencedirect.com/journal/international-journal-of-pharmaceutics-x

Feed factor profile prediction model for two-component mixed powder in the twin-screw feeder

Yuki Kobayashi [a], Sanghong Kim [b], Takuya Nagato [c], Takuya Oishi [c,d], Manabu Kano [a,*]

[a] Department of Systems Science, Kyoto University, Yoshida-honmachi, Sakyo-ku, Kyoto 6068501, Kyoto, Japan
[b] Department of Applied Physics and Chemical Engineering, Tokyo University of Agriculture and Technology, 2-24-16 Naka-cho, Koganei, 1840012 Tokyo, Japan
[c] Research and Development Division, Powrex Corporation, 5-5-5 Kitagawara, Itami 6640837, Hyogo, Japan
[d] Department of Applied Chemistry, Tokyo University of Agriculture and Technology, 2-24-16 Naka-cho, Koganei, 1840012 Tokyo, Japan

ARTICLE INFO

Keywords:
Feed factor profile
Loss-in-weight feeder
Continuous manufacturing
Material properties
Mixed powder
Prediction model

ABSTRACT

In continuous pharmaceutical manufacturing processes, it is crucial to control the powder flow rate. The feeding process is characterized by the amount of powder delivered per screw rotation, referred to as the feed factor. This study aims to develop models for predicting the feed factor profiles (FFPs) of two-component mixed powders with various formulations, while most previous studies have focused on single-component powders. It further aims to identify the suitable model type and to determine the significance of material properties in enhancing prediction accuracy by using several FFP prediction models with different input variables. Four datasets from the experiment were generated with different ranges of the mass fraction of active pharmaceutical ingredients (API) and the powder weight in the hopper. The candidates for the model inputs are (a) the mass fraction of API, (b) process parameters, and (c) material properties. It is desirable to construct a high-performance prediction model without the material properties because their measurement is laborious. The results show that using (c) as input variables did not improve the prediction accuracy as much, thus there is no need to use them.

1. Introduction

In the pharmaceutical industry, maintaining high product quality and reducing the cost of R&D and manufacturing are essential. Since the 2000s, there has been an increasing interest in product quality prediction models and continuous manufacturing to satisfy these needs (Ierapetritou et al., 2016). Continuous manufacturing has several advantages over batch manufacturing, such as smaller equipment size, elimination of scale-up, and reduced operator numbers (Lee et al., 2015). In the continuous manufacturing processes of pharmaceutical products, it is essential to control the feed rate of the raw materials at its set point to produce uniform products since the fluctuation of the feed flow rate can be propagated to downstream processes and can deteriorate product quality (Blackshields and Crean, 2018; Suzuki et al., 2021).

In the powder feeding processes, screw feeders are commonly used (Blackshields and Crean, 2018; Engisch and Muzzio, 2015b). A screw feeder has a hopper and one or two screws by which the powder in the hopper is extruded. The screw feeder is set on the weighing scale and has a controller to keep the flow rate at its set point. This type of feeder is called a loss-in-weight (LIW) feeder. The flow rate is calculated from the change in powder weight in the hopper. Then, the screw rotation speed is manipulated so that the calculated flow rate follows the set point. When the flow rate cannot be calculated accurately, such as when refilling the hopper with powder, the screw is usually operated at a constant rotational speed (Blackshields and Crean, 2018).

Many studies on LIW feeders were conducted for experimental and modeling aspects. The methods of measuring the feeding performance at steady state (Engisch and Muzzio, 2012) and during hopper refill (Engisch and Muzzio, 2015a) were presented and demonstrated. The feeding performance of components of a formulation for continuous direct compression was examined, and the challenges were resolved (Engisch and Muzzio, 2015b). In addition to experimental studies, various modeling studies were conducted. Particle scale simulations were carried out using the discrete element method (DEM) (Hou et al., 2014; Bhalode and Ierapetritou, 2020). The mixing behaviors in the feeder were modeled by residence time distribution modeling (Van Snick et al., 2019; Waeytens et al., 2022). Physical models with lumped parameters were developed based on the pressure exerted by the powder in the hopper and powder extrusion by the screw (Wang et al., 2017b; Bascone et al., 2020). The parameters have to be determined by

* Corresponding author.
E-mail address: manabu@human.sys.i.kyoto-u.ac.jp (M. Kano).

https://doi.org/10.1016/j.ijpx.2024.100242
Received 8 October 2023; Received in revised form 14 March 2024; Accepted 28 March 2024
Available online 31 March 2024

Table 1
Literature survey results on FF/FFP prediction models.

Literature	Feeding mixture	Changing formulation	Predicting FFP	Model	Investigating the necessity of material properties
Pordesimo et al. (2009)				MLR	
Yadav et al. (2019)				PLS	
Bostijn et al. (2019)				PLS	
Stauffer et al. (2019)	✓			PLS	
Tahir et al. (2020)			✓	PLS	
Bekaert et al. (2021)				PLS	
Shier et al. (2022)			✓	PM + SVR	
This study	✓	✓	✓	7 models	✓

The 7 models in this study include PLS, RF, GPR, PM + PLS, PM + RF, SLR + PLS, and SLR + RF.

experimental data for each powder. Chen and Ierapetritou (2020); Shier et al. (2022) developed gray-box models based on Heckel's equation (Heckel, 1961) based physical model proposed by (Wang et al., 2017b). The statistical models were developed to link the feeding performance with material properties, process parameters, and feeder configurations (Jia et al., 2009; Pordesimo et al., 2009; Wang et al., 2017a; Santos et al., 2018; Escotet-Espinoza et al., 2018; Wang et al., 2019; Bostijn et al., 2019; Stauffer et al., 2019; Yadav et al., 2019; Tahir et al., 2020; Bekaert et al., 2021).

The feeding performance can suffer from challenges such as a low flow rate set point, powder cohesiveness, refilling the hopper with powder, and changing the set point. Mixed powder has advantages over single-component powder as feed in three situations (Oka et al., 2017). The first is when the flow rate set point is low. For example, if the mass fraction of API is small, the flow rate would be small. The performance of the screw feeder often degrades at a low flow rate. In this case, feeding mixed powder enables a larger set point for the flow rate and reduces flow rate fluctuations (Kerins and Crean, 2022). The second is when the number of components in a product is large. In this case, the number of feeders can be reduced by using mixed powder. The third is when a component is highly cohesive such as acetaminophen. In this case, feeding mixed powder may improve flowability.

For a long-term operation, refilling the hopper with powder is needed. The set point of flow rate can be changed to control API concentration (Hanson, 2018; Kirchengast et al., 2019), the flow rate from the mixer (Singh et al., 2013), or the powder level in the hopper before the tablet press (Kirchengast et al., 2019). During the refill or at the set point change, the screw rotational speed has to be appropriately manipulated to keep the flow rate at the set point. Feed factor profile (FFP) prediction models are useful for achieving this objective. A feed factor f [g] is the amount of powder fed per screw rotation (Shier et al., 2022). The relationship between the feed factor and the powder weight in the hopper is called the feed factor profile (Shier et al., 2022).

We surveyed literature that built feed factor prediction models for various powders, and summarized in Table 1. While most past research focused on feeding single-component powder, this study focuses on feeding mixed powder. Moreover, in this study, the formulation of mixed powder was changed, and thus the models can use the formulation as input variables. This makes it possible to use the models for optimizing the number of feeders and formulation of the mixture in each feeder. This study aims to predict FFP rather than a single feed factor, e.g., a feed factor at only one condition such as when the hopper is fully occupied with powder. Modeling FFP is more complex but can help to ensure the stable operation for a wider range of the powder weight in the hopper.

In other studies working on the prediction of FFP, many experiments using various kinds of powder materials were conducted for model development. For example, Tahir et al. (2020) conducted 224 experiments. They also assume large databases of material properties. This approach applies to the prediction of FFP for a wide range of materials but is not realistic for small companies due to their small budgets. Our study takes another approach focusing on how to develop FFP prediction models for mixed powder composed of specific materials. In some cases, this approach is less expensive because it requires neither large preliminary experiments nor databases.

The modeling process in this study is thorough. This study compares seven models because the prediction of FFP of the multi-component mixture should be more difficult than the prediction of FFP of single-component powders or a single feed factor of single-component powders. The abbreviations for the model names used in this paper are as follows: partial least squares (PLS), random forest (RF), gaussian process regression (GPR), physical model (PM), simple linear regression (SLR), multiple linear regression (MLR), and support vector regression (SVR). A two-step approach is adopted when using either PM or SLR. For example, PM + PLS is the denotion of the model which combines PM and PLS.

Material properties may help to predict FFP or FF, but the sample preparation and measurement are laborious. If a model incorporating material properties into its input variable set only shows marginal improvement in prediction accuracy, then the measurement of these properties can be deemed unnecessary. As such, this study compares two input variable sets: the first comprises formulation parameters and process parameters, while the second includes formulation parameters, process parameters, and material properties of mixed powder.

The contributions of this work are that we have developed models for predicting FFP of mixed powders for the first time, we investigated the difference of prediction accuracy of the models, and that the material properties of mixed powders are not necessarily required for accurate FFP prediction. To achieve this, the feeding experiments of mixed powder were conducted by changing the mass fractions of API and the powder weight in the hopper. After the experiments, seven FFP prediction models were built and compared with four model building datasets in which the ranges of input variables are different.

The structure of this paper is as follows. Section 2 describes the experimental and model building method. Section 3 describes the experimental and model building results. Section 4 presents the conclusions.

Table 2
Experimental conditions: experiment number (#Exp), mass fraction of ethenzamide (X_{API}), and screw rotation speed (ω).

#Exp	X_{API} [−]	ω [rpm]
1–1	0.01	18.8
1–2	0.01	37.8
1–3	0.01	37.8
2–1	0.02	19.1
2–2	0.02	38.2
2–3	0.02	38.2
3–1	0.03	18.0
3–2	0.03	36.2
4–1	0.05	17.8
4–2	0.05	35.9
5–1	0.07	17.6
5–2	0.07	35.6
6–1	0.10	17.6
6–2	0.10	35.5

Table 3
Measured material properties.

Material property	Unit
D_{10}, D_{50}, D_{90}	μm
Tapped bulk density	g/cm^3
Aerated bulk density	g/cm^3
Compressibility	–
Hausner ratio	–
Angle of repose	degree
Angle of rupture	degree
Angle of difference	degree
Angle of spatula	degree
Degree of agglomeration	%
Degree of dispersion	%
Flowability index	–
Floodability index	–

2. Materials and methods

2.1. Experiments

In the experiments, twin screw feeder (TSF), LIW-300-P (Ishida, Japan), was used. Ethenzamide (Iwaki Seiyaku, Japan) was used as an API, and spray-dried lactose (DFE Pharma, Germany) was used as an excipient. Ethenzamide was selected as the model drug because it is safe and popular.

Six types of powder mixtures in Table 2 were prepared. Each mixture was fed into the hopper of the feeder. The feeder was operated at the screw rotation speed in Table 2 until no powder came out of the feeder outlet, and operating data of process parameters such as powder weight in the hopper and flow rate were obtained. The material properties of the six mixtures in Table 3 were measured.

The particle size distribution was measured and the representative values of the distribution, D_{10}, D_{50}, and D_{90}, were calculated by Particle Viewer (Powrex, Japan). The diameters of 10, 50, and 90% of the particles are below these values, respectively. Other material properties were measured using the Powder Tester PT-S (Hosokawa micron, Japan). PT-S was used according to the procedure indicated by the accompanying software. Aerated bulk density ρ_A and tapped bulk density ρ_P were measured using a 100 mL cylinder. The compressibility C was calculated from ρ_A and ρ_P using Eq. (1).

$$C = \frac{\rho_P - \rho_A}{\rho_P} \tag{1}$$

Angle of repose is the angle formed between the table and the slope of the mountain formed when the sample was placed on a sieve with an aperture of 710 μm, the sieve was vibrated, and the sample was dropped from a roto set under the sieve onto a table. After the measurement of angle of repose, angle of rupture was measured as the angle formed by the slope and the table after the mountain ruptured due to the impact on the table on which the powder was placed. Angle of difference was the difference between the angle of repose and the angle of rupture. Angle of spatula is the average of the angle formed by the slope and the flat plate when the powder is piled on a horizontal flat plate and the flat plate is moved directly up, and the angle formed by the slope and the flat plate after an impact is applied to the flat plate. Measurements were taken three times and averaged. Degree of agglomeration was determined from the amount of powder remaining on the 250, 150, and 75 μm sieves. Degree of dispersion was determined by weighing the powder weight remaining in a dish placed at the drop point when 10 g of powder was dropped, and the percentage of the powder dispersed was calculated. Measurements were taken three times and averaged. The flowability index and floodability index are indices proposed by Carr (1965) and determined using the proposed tables.

Table 4
Model building datasets with different ranges of the powder weight in the hopper (W) and the ethenzamide mass fraction (X_{API}).

Dataset	W [kg]	X_{API} [−]
1	1.0–3.0	0.03–0.10
2	0.5–3.5	0.03–0.10
3	1.0–3.0	0.01–0.10
4	0.5–3.5	0.01–0.10

2.2. Modeling

2.2.1. Feed factor calculation

The feed factor f [g] was calculated using the flow rate F [g/min] and the screw rotation speed ω [rpm] (Tahir et al., 2020). F is the instantaneous flow rate and calculated every second.

$$f = \frac{F}{\omega} \tag{2}$$

2.2.2. Model descriptions

PLS (Geladi and Kowalski, 1986), RF (Breiman, 2001), GPR (Rasmussen and Williams, 2005), PM, and SLR are used in this study. PLS is a linear regression method that can handle multi-collinearity, and it is widely used in spectroscopic analysis to construct calibration models. RF and GPR can handle nonlinearities in the relationship between output and input variables; RF uses bagging (bootstrap aggregating) and decision-trees, while GPR uses kernel functions. They have the advantage of being able to handle complex nonlinearities, but optimizing hyper-parameters is difficult and time-consuming. These methods, i.e., PLS, RF, and GPR, are data-driven. On the other hand, the physical model is derived from the first principles on the target process and materials. It can describe the nonlinear relationship between the feed factor and the powder weight in the hopper. However, it is difficult to accurately represent complex phenomena using only physical models, and it is often necessary to combine them with statistical models. Such combined models are called gray-box models (Ahmad et al., 2014). SLR assumes that the relationship between the feed factor and the powder weight in the hopper is linear, and it can be combined with nonlinear models representing the relationship between the parameters of SLR and input variables other than the powder weight in the hopper.

Eq. (3) was used for the kernel function composed of constant kernel, RBF kernel, and white kernel (Rasmussen and Williams, 2005).

$$k(\boldsymbol{x}_n, \boldsymbol{x}_{n'}) = cexp\left(-\frac{d(\boldsymbol{x}_n, \boldsymbol{x}_{n'})^2}{2l^2}\right) + w(\boldsymbol{x}_n, \boldsymbol{x}_{n'}) \tag{3}$$

where $\boldsymbol{x}_n$ is the input variable vector of the n^{th} sample, $d(\boldsymbol{x}_n, \boldsymbol{x}_{n'})$ is the Euclidean distance between $\boldsymbol{x}_n$ and $\boldsymbol{x}_{n'}$, $w(\boldsymbol{x}_n, \boldsymbol{x}_{n'})$ is the white kernel, which returns σ when $n = n'$ and 0 otherwise, and c [−], l [−] and σ [−] are constants.

The physical model is Eq. (4) (Wang et al., 2017b), which is based on Heckel's equation (Heckel, 1961).

$$f(W) = \alpha - (\alpha - \beta)exp(-\gamma W) \tag{4}$$

where W [g] is the powder weight in the hopper, α [g], β [g], and γ [g^{-1}] are the maximum, minimum, and rate of decay in f, respectively.

The SLR model is Eq. (5).

$$f(W) = aW + b \tag{5}$$

where a [−] and b [g] are the regression coefficients.

2.2.3. Model building methods

As will be discussed later, it was anticipated from the experimental results that the appropriate model would differ depending on the range of the ethenzamide mass fraction and the range of the powder weight in

Table 5
Four variable groups (VGs) including variables initially putted into the input variable set S: powder weight in the hopper (W), screw rotation speed (ω), ethenzamide mass fraction (X_{API}), and material properties (Props).

VG	W	ω	X_{API}	Props
1	✓	✓	✓	✓
1	✓	✓	✓	
3		✓	✓	✓
4		✓	✓	

the hopper. Therefore, four model-building datasets in Table 4 were defined and seven models were constructed for each dataset. As shown in Table 2, two or three experiments were conducted for each mass fraction of ethenzamide. In the model building, experimental data with the same ethenzamide mass fraction are treated as one group. As a result, there are six groups.

The root mean squared error (RMSE), the maximum error (ME), and the mean absolute percentage error (MAPE) were used as the criterion for model evaluation.

$$\mathrm{RMSE} = \sqrt{\frac{1}{N}\sum_{n=1}^{N}(y_n - \hat{y}_n)^2} \tag{6}$$

$$\mathrm{ME} = max(|y_1 - \hat{y}_1|, \ldots, |y_N - \hat{y}_N|) \tag{7}$$

$$\mathrm{MAPE} = \frac{100}{N}\sum_{n=1}^{N}\left|\frac{y_n - \hat{y}_n}{y_n}\right| \tag{8}$$

where y_n is the n^{th} measured value, $\hat{y}_n$ is the its predicted value, and N is the number of samples. ME is used as well as RMSE because it is necessary to consider not only the average error but also the maximum error.

The procedure to build PLS, RF, and GPR models is as follows:

(1) Select a model from PLS, RF, and GPR.
(2) Select whether to use the material properties or not.
(3) Put variables into the input variable set S. If the material properties are used, put variables in VG1 in Table 5 into S. Otherwise, put variables in VG2 into S.
(4) Build a model using leave one-group out cross-validation (LOGOCV).
(5) Calculate the mean of RMSEs and the means of MEs in the cross-validation, which are referred to as RMSECV and MECV.
(6) Calculate the mean of permutation importance (PI) (Altmann et al., 2010) in the cross-validation, which is referred to as PICV.
(7) Exclude the input variable with the smallest PICV from S.
(8) Perform steps (4) through (7) until S becomes empty.
(9) Select S of the model with the smallest RMSECV.
(10) Perform steps (2) through (9), changing the selection in step (2).
(11) Perform steps (1) through (10), changing the selection in step (1).

In step (4), hyperparameters were optimized. In PLS, the number of latent variables was determined by nested LOGOCV. In RF, the number of trees was determined by nested LOGOCV. In GPR, the parameters of the kernel function were determined by non-nested LOGOCV and maximum likelihood estimation. The dataset was standardized before the regression in PLS and GPR.

The procedure to build PM + PLS, PM + RF, SLR + PLS, and SLR + RF models is as follows:

(i) Calculate the parameters in Eqs. (4) or (5) so that the sum of squared errors between the actual and predicted feed factors is minimized.
(ii) Build a PLS or RF model whose output variable is the calculated parameters with the same steps (1) through (11) except for steps (1) and (3). In step (1), select a model from PLS and RF. In step (3), put variables in VG3 in Table 5 into S if the material properties are used, and put variables in VG4 in Table 5 into S the material properties are not used.

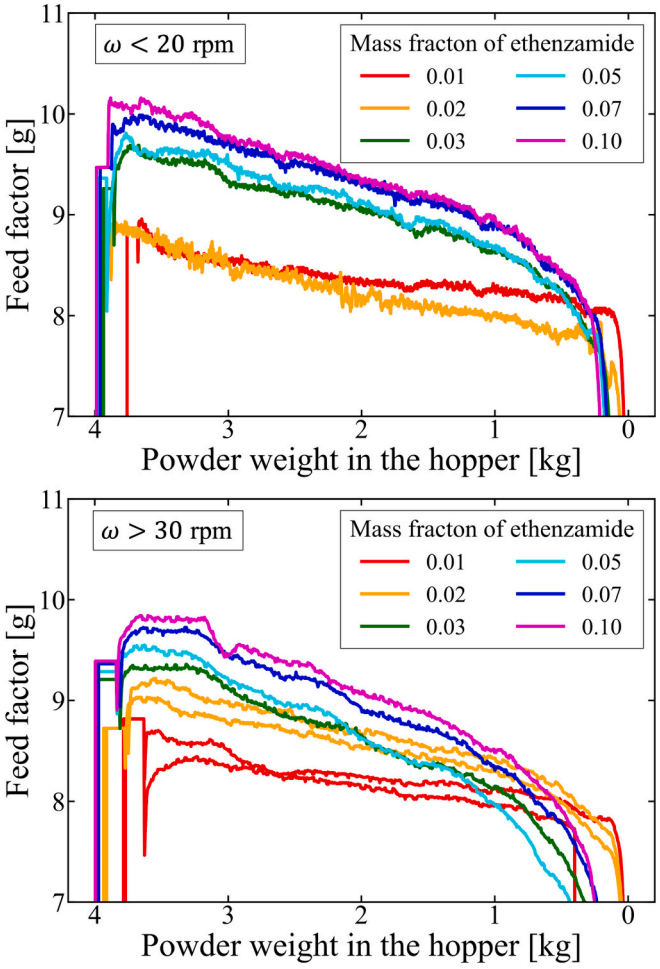

Fig. 1. Relationship between feed factor and powder weight in the hopper, when the screw rotation speed is below 20 rpm (top) and above 30 rpm (bottom).

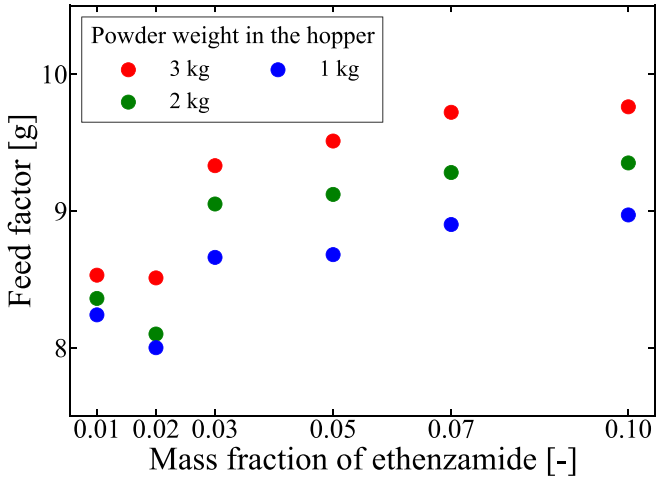

Fig. 2. Relationship between feed factor and mass fraction of ethenzamide when the screw rotaton speed is below 20 rpm.

Table 6
RMSECVs of seven models, with or without material properties as input variables, for four datasets in Table 4.

Model	With material properties				Without material properties			
	Dataset 1	Dataset 2	Dataset 3	Dataset 4	Dataset 1	Dataset 2	Dataset 3	Dataset 4
PLS	**0.071**	**0.118**	0.224	0.259	0.105	0.142	0.279	0.307
RF	0.115	0.120	0.188	0.224	0.115	**0.122**	0.273	0.290
GPR	0.226	0.220	0.202	0.408	**0.098**	0.123	0.485	0.495
PM + PLS	0.149	0.144	0.332	0.221	0.212	0.140	0.303	0.305
PM + RF	0.167	0.177	0.224	0.207	0.136	0.187	0.250	0.288
SLR + PLS	0.093	0.124	0.216	0.307	**0.098**	0.137	0.284	0.327
SLR + RF	0.147	0.138	**0.186**	**0.205**	0.136	0.153	**0.237**	**0.268**

The bolded number is the smallest RMSECV for each dataset.

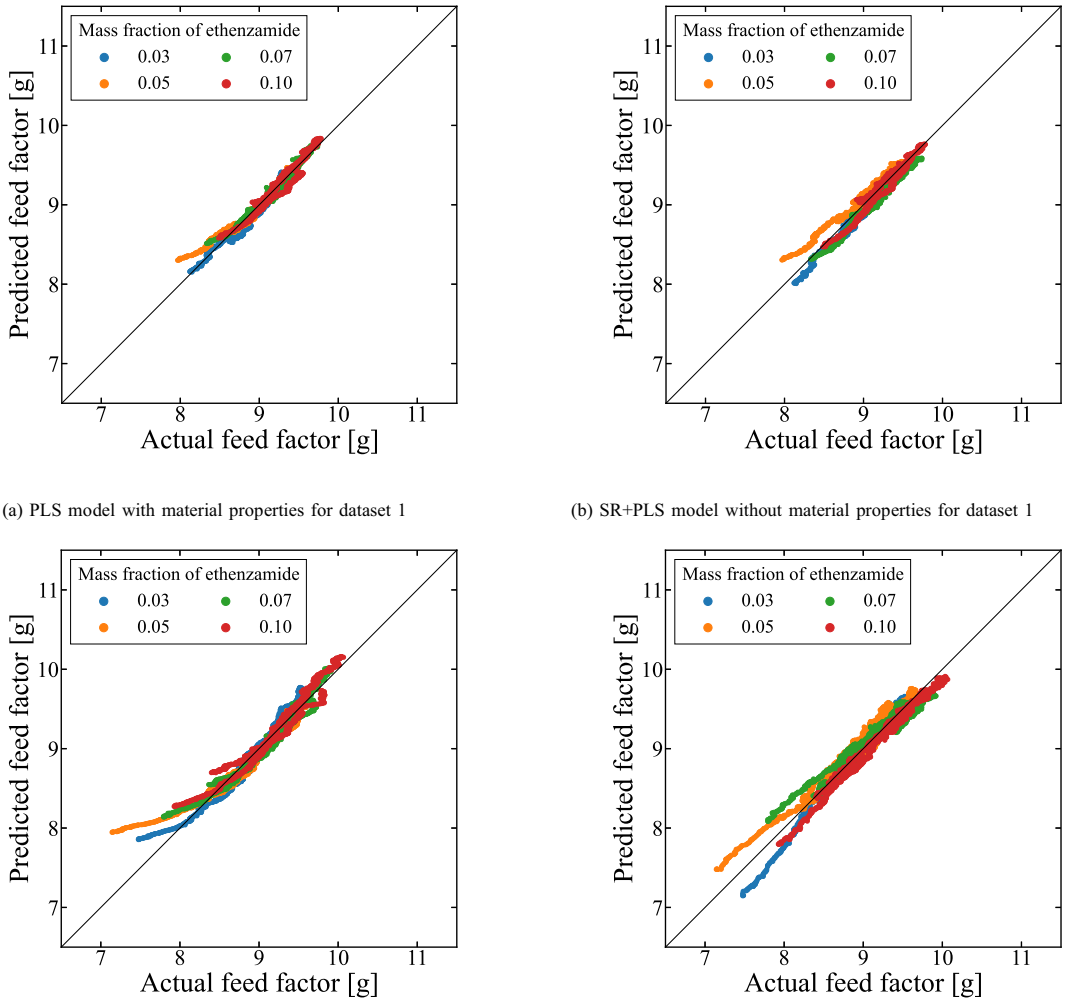

(a) PLS model with material properties for dataset 1

(b) SR+PLS model without material properties for dataset 1

(c) PLS model with material properties for dataset 2

(d) RF model without material properties for dataset 2

Fig. 3. Prediction results of feed factors using the models with the smallest RMSECVs for four datasets, with or without material properties.

3. Results and discussions

3.1. Experimental results

Fig. 1 illustrates the relationship between the powder weight in the hopper and the feed factor, i.e. FFP, under different conditions of screw rotation speed and mass fraction of ethenzamide. Fig. 1 (top) shows FFP when the screw rotation speed is below 20 rpm, while Fig. 1 (bottom) presents FFP when the screw rotation speed is above 30 rpm. The feed factor almost linearly decreases with powder weight in the hopper for the range of the powder weight in the hopper of 1.0–3.0 kg, but more nonlinearity is observed when this range expands to 0.5–3.5 kg. As the powder weight in the hopper decreases, the pressure at the bottom of the hopper decreases and the density of the powder decreases. The possible reasons for this nonlinearity are that the rate at which the density decreases depends on the powder weight in the hopper, or the ease of powder flow into the screw section depends on the amount of powder in the hopper. Fig. 2 shows the relationship between the mass fraction of ethenzamide and the feed factor when the powder weight in the hopper is 1, 2, or 3 kg. The feed factor almost linearly decreases with the mass

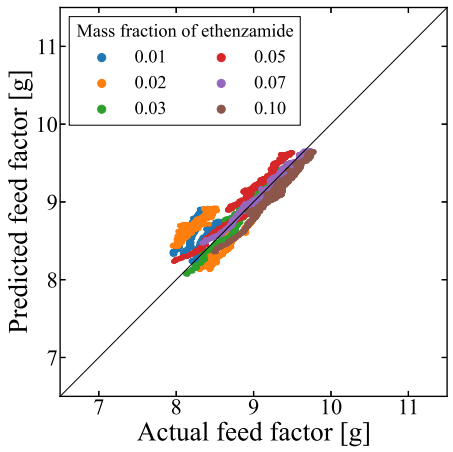

(e) SLR+RF model with material properties for dataset 3

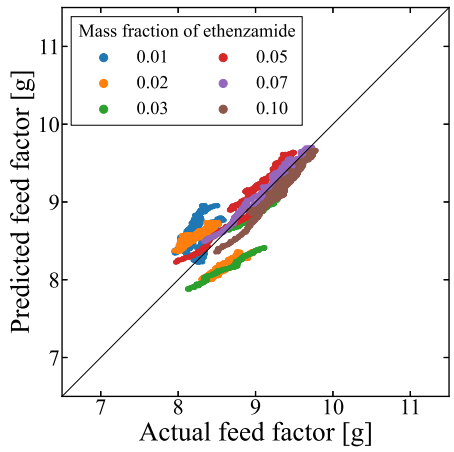

(f) SLR+RF without material properties for dataset 3

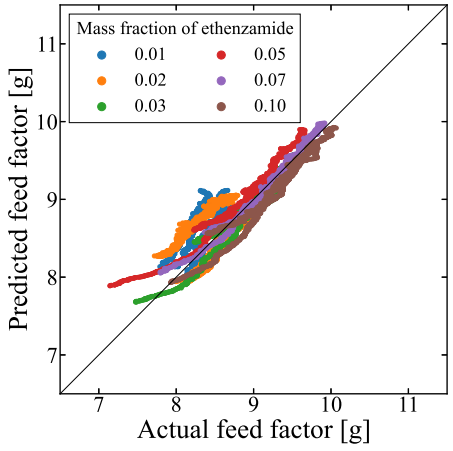

(g) SLR+RF model with material properties for dataset 4

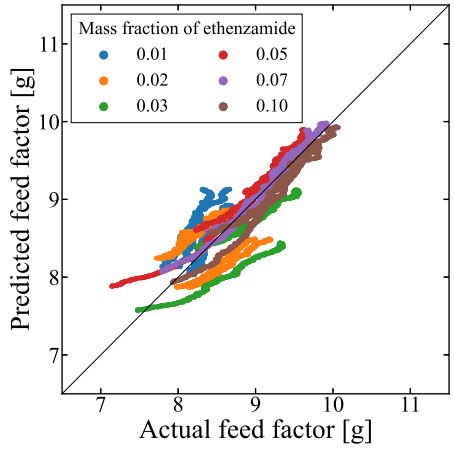

(h) SLR+RF model without material properties for dataset 4

Fig. 3. (*continued*).

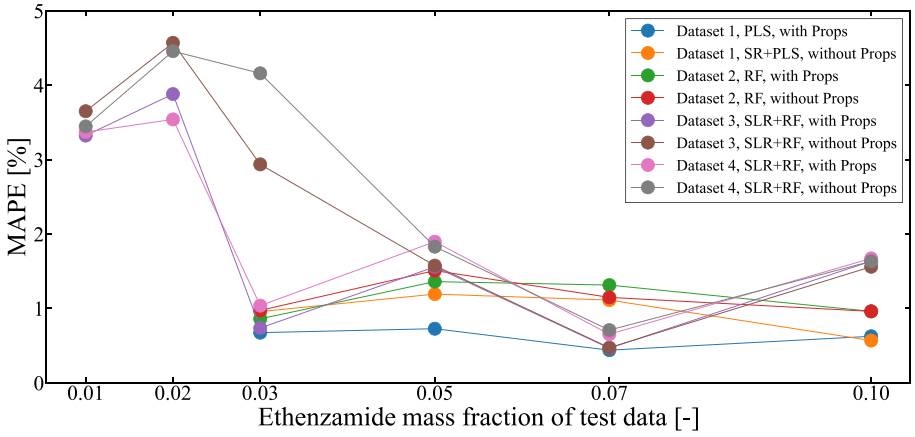

Fig. 4. MAPEs for the test data in cross-validation for four datasets, with or without material properties (Props). All MAPEs are below 5%.

fraction of ethenzamide when the mass fraction of ethenzamide is in the range of 0.03–0.10, but the nonlinearity increases when it is expanded to 0.01–0.10. The results suggest that linear models predicting feed factor are appropriate when the range of powder weight in the hopper is 1.0–3.0 kg, and that of ethenzamide mass fraction is 0.3–1.0. To check this hypothesis, we created four datasets in Table 4.

3.2. Modeling results

RMSECVs of all models are summarized in Table 6. For each dataset (1, 2, 3, or 4), the difference in the smallest RMSECVs achieved by the models with and without material properties was less than 0.1 g, which is a small improvement considering the cost of measuring the material

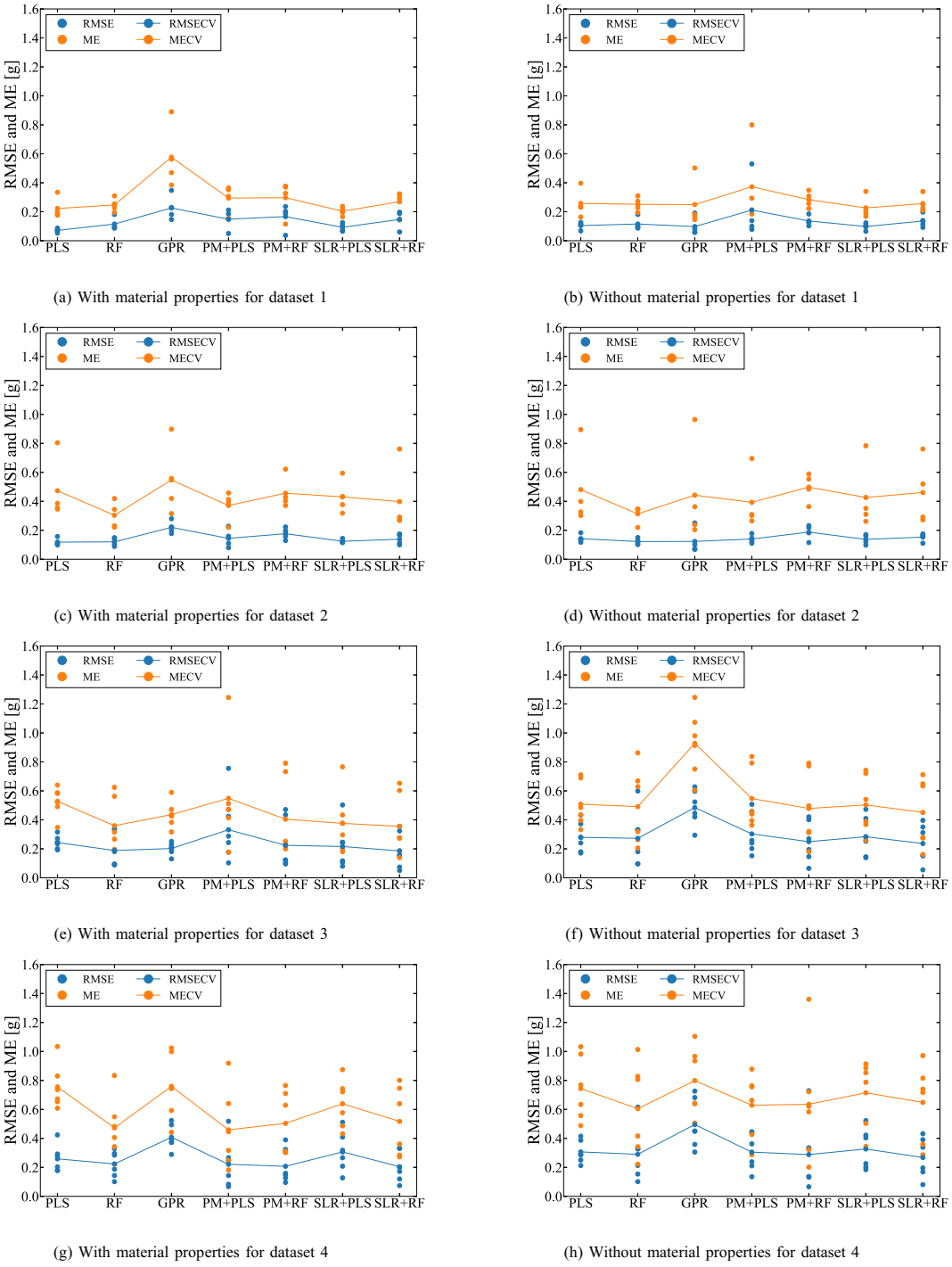

(a) With material properties for dataset 1

(b) Without material properties for dataset 1

(c) With material properties for dataset 2

(d) Without material properties for dataset 2

(e) With material properties for dataset 3

(f) Without material properties for dataset 3

(g) With material properties for dataset 4

(h) Without material properties for dataset 4

Fig. 5. Comparison of prediction accuracy of seven models using RMSE, ME, RMSECV, and MECV.

properties. Focusing on dataset 2, for example, the PLS model achieved the smallest RMSECV of 0.118 g using material properties, and the RF model achieved the smallest RMSECV of 0.122 g not using material properties. The difference is only 0.004 g. It is not worth the measurement cost to use the material properties as input variables of the prediction model. Fig. 3 shows the actual and predicted feed factors using the models with the smallest RMSECVs for four datasets with or without material properties. Fig. 3 (a)-(h) shows that the plots of actual and predicted feed factors are generally on the diagonal, which indicates that the prediction is successful.

Fig. 4 shows MAPEs for the test data in the cross-validation, with or without material properties. All MAPEs are below 5%. Shier et al. (2022) reported that the median of MAPEs of feed factors was below 10%, which demonstrated the model's good predictive capability. Chen and Ierapetritou (2020) predicted flow rates by multiplying the feed factor by the screw rotation speed and reported that MAPEs were reduced from 17.78% with the white-box model to 9% with the gray-box model. In the present study, the screw rotation speed was constant during each experiment; thus, MAPEs of feed factors are the same as those of the flowrate according to Eq. (8). MAPEs in this study are not directly comparable to these results because the datasets are different; however, the models constructed in this study, whose MAPEs are below 5%, are considered to have good predictive capability regardless of using material properties.

In discussing absolute rather than relative errors, Shier et al. (2022) stated that the goal was ideally to achieve prediction errors of feed factors within 0.1 g. Tahir et al. (2020) considered prediction errors of feed factors of 0.25–0.43 g high and successfully reduced the predictive errors to 0.10–0.17 g by constructing models for clusters of powders with similar material properties. However, the absolute values of feed factors in the present study are significantly larger than those of other studies, and the acceptable absolute errors become larger. In practice, the acceptable prediction error depends on the influence of the prediction error on the final product quality. Thus, the assessment with downstream unit operations should be conducted as flow sheet models (Galbraith et al., 2020, 2019; Tian et al., 2019; García-Muñoz et al., 2018) or experiments (Karttunen et al., 2020).

In this study, the PLS models achieved small RMSECVs for datasets 1 and 2, both with and without material properties. This result suggests that PLS was enough for datasets with a narrow range of ethenzamide mass fractions. The SLR + RF models achieved the smallest RMSECV for datasets 3 and 4, both with and without material properties, which indicates that considering the nonlinearity between ethenzamide mass fraction and the parameters of SLR improved the prediction accuracy. MAPE of 10% corresponds to just under 1 g of RMSECV in this study. As shown in Table 6, RMSECVs are generally around 0.2 g, indicating that a sufficiently high prediction accuracy was achieved. Fig. 5 displays RMSEs and MEs for each model for each test data in the cross-validation. For example, in dataset 4, where the model has a wider range of applicability, although the SLR + RF model achieved the smallest RMSECV, it is difficult to conclude it is the best model because the difference in RMSECV for each model is not significant enough for the range of its variability.

4. Conclusions

Models were constructed to predict the feed factor profile (FFP) of the mixed powders. Multiple models were evaluated across four datasets, each with different ranges of ethenzamide mass fractions and powder weight in the hopper. Although the difference in RMSECV among models was not significant, the SLR + RF model achieved the best prediction performance for the dataset with wide ranges of the mass fraction of ethenzamide and the powder weight in the hopper. To the extent examined in this study, compared to models whose inputs are only the mass fraction of ethenzamide, powder weight in the hopper, and screw rotation speed, models which additionally included material properties such as bulk density and angle of repose did not improve prediction accuracy as much. Thus, incorporating material properties as input variables is not deemed essential to predict FFP. In the future, the raw materials will be changed to confirm the generality of the conclusions. In addition, we plan to examine mixtures with three or more components.

CRediT authorship contribution statement

Yuki Kobayashi: Writing – review & editing, Writing – original draft, Visualization, Validation, Software, Methodology, Investigation, Formal analysis, Data curation, Conceptualization. **Sanghong Kim:** Writing – review & editing, Methodology, Investigation, Conceptualization. **Takuya Nagato:** Writing – review & editing, Validation, Resources, Project administration, Methodology, Investigation, Conceptualization. **Takuya Oishi:** Writing – review & editing, Validation, Resources, Methodology, Investigation, Data curation, Conceptualization. **Manabu Kano:** Writing – review & editing, Resources, Methodology, Funding acquisition, Conceptualization.

Declaration of competing interest

There is no Conflict of Interest.

Data availability

The data that has been used is confidential.

Acknowledgements

This work was supported by Japan Science and Technology Agency (JST), the establishment of university fellowships towards the creation of science technology innovation, Grant Number JPMJFS2123 and by Japan Society for the Promotion of Science (JSPS) KAKENHI Grant Number JP21H01704. Kazuhiro Uchida, Kazuyoshi Kotaka, Kazuya Tanabe, Kenji Hirata, and Koji Tabayashi from Powrex Corporation are gratefully acknowledged for their data collection support.

References

Ahmad, I., Kano, M., Hasebe, S., Kitada, H., Murata, N., 2014. Gray-box modeling for prediction and control of molten steel temperature in tundish. J. Process Control 24, 375–382. https://doi.org/10.1016/j.jprocont.2014.01.018.

Altmann, A., Toloşi, L., Sander, O., Lengauer, T., 2010. Permutation importance: a corrected feature importance measure. Bioinformatics 26, 1340–1347. https://doi.org/10.1093/bioinformatics/btq134.

Bascone, D., Galvanin, F., Shah, N., Garcia-Munoz, S., 2020. Hybrid Mechanistic-Empirical approach to the modeling of twin screw feeders for continuous tablet manufacturing. Ind. Eng. Chem. Res. 59, 6650–6661. https://doi.org/10.1021/acs.iecr.0c00420.

Bekaert, B., Penne, L., Grymonpré, W., Van Snick, B., Dhondt, J., Boeckx, J., Vogeleer, J., De Beer, T., Vervaet, C., Vanhoorne, V., 2021. Determination of a quantitative relationship between material properties, process settings and screw feeding behavior via multivariate data-analysis. Int. J. Pharm. 602, 120603 https://doi.org/10.1016/j.ijpharm.2021.120603.

Bhalode, P., Ierapetritou, M., 2020. Discrete element modeling for continuous powder feeding operation: Calibration and system analysis. Int. J. Pharm. 585, 119427 https://doi.org/10.1016/j.ijpharm.2020.119427.

Blackshields, C.A., Crean, A.M., 2018. Continuous powder feeding for pharmaceutical solid dosage form manufacture: a short review. Pharm. Dev. Technol. 23, 554–560. https://doi.org/10.1080/10837450.2017.1339197.

Bostijn, N., Dhondt, J., Ryckaert, A., Szabó, E., Dhondt, W., Van Snick, B., Vanhoorne, V., Vervaet, C., De Beer, T., 2019. A multivariate approach to predict the volumetric and gravimetric feeding behavior of a low feed rate feeder based on raw material properties. Int. J. Pharm. 557, 342–353. https://doi.org/10.1016/j.ijpharm.2018.12.066.

Breiman, L., 2001. Random forests. Mach. Learn. 45, 5–32. https://doi.org/10.1023/A:1010933404324.

Carr, R.L., 1965. Evaluating flow properties of solids. Chem. Eng. 72, 163–168.

Chen, Y., Ierapetritou, M., 2020. A framework of hybrid model development with identification of plant-model mismatch. AICHE J. 66 https://doi.org/10.1002/aic.16996.

Engisch, W.E., Muzzio, F.J., 2012. Method for characterization of loss-in-weight feeder equipment. Powder Technol. 228, 395–403. https://doi.org/10.1016/j.powtec.2012.05.058.

Engisch, W.E., Muzzio, F.J., 2015a. Feedrate deviations caused by hopper refill of loss-in-weight feeders. Powder Technol. 283, 389–400. https://doi.org/10.1016/j.powtec.2015.06.001.

Engisch, W.E., Muzzio, F.J., 2015b. Loss-in-weight feeding trials case study: Pharmaceutical formulation. J. Pharm. Innov. 10, 56–75. https://doi.org/10.1007/s12247-014-9206-1.

Escotet-Espinoza, M.S., Moghtadernejad, S., Scicolone, J., Wang, Y., Pereira, G., Schäfer, E., Vigh, T., Klingeleers, D., Ierapetritou, M., Muzzio, F.J., 2018. Using a material property library to find surrogate materials for pharmaceutical process development. Powder Technol. 339, 659–676. https://doi.org/10.1016/j.powtec.2018.08.042.

Galbraith, S.C., Cha, B., Huang, Z., Park, S., Liu, H., Meyer, R.F., Flamm, M.H., Hurley, S., Zhang-Plasket, F., Yoon, S., 2019. Integrated modeling of a continuous direct compression tablet manufacturing process: a production scale case study. Powder Technol. 354, 199–210. https://doi.org/10.1016/j.powtec.2019.05.078.

Galbraith, S.C., Park, S., Huang, Z., Liu, H., Meyer, R.F., Metzger, M., Flamm, M.H., Hurley, S., Yoon, S., 2020. Linking process variables to residence time distribution in a hybrid flowsheet model for continuous direct compression. Chem. Eng. Res. Des. 153, 85–95. https://doi.org/10.1016/j.cherd.2019.10.026.

García-Muñoz, S., Butterbaugh, A., Leavesley, I., Manley, L.F., Slade, D., Bermingham, S., 2018. A flowsheet model for the development of a continuous process for pharmaceutical tablets: an industrial perspective. AICHE J. 64, 511–525. https://doi.org/10.1002/aic.15967.

Geladi, P., Kowalski, B.R., 1986. Partial least-squares regression: a tutorial. Anal. Chim. Acta 185, 1–17. https://doi.org/10.1016/0003-2670(86)80028-9.

Hanson, J., 2018. Control of a system of loss-in-weight feeders for drug product continuous manufacturing. Powder Technol. 331, 236–243. https://doi.org/10.1016/j.powtec.2018.03.027.

Heckel, R.W., 1961. Density-pressure relationships in powder compaction. Trans. Metall. Soc. AIME 221, 671–675.

Hou, Q.F., Dong, K.J., Yu, A.B., 2014. DEM study of the flow of cohesive particles in a screw feeder. Powder Technol. 256, 529–539. https://doi.org/10.1016/j.powtec.2014.01.062.

Ierapetritou, M., Muzzio, F., Reklaitis, G., 2016. Perspectives on the continuous manufacturing of powder-based pharmaceutical processes. AICHE J. 62, 1846–1862. https://doi.org/10.1002/aic.15210.

Jia, Z., Davis, E., Muzzio, F.J., Ierapetritou, M.G., 2009. Predictive modeling for pharmaceutical processes using kriging and response surface. J. Pharm. Innov. 4, 174–186. https://doi.org/10.1007/s12247-009-9070-6.

Karttunen, A.P., Poms, J., Sacher, S., Sparén, A., Ruiz Samblás, C., Fransson, M., Martin De Juan, L., Remmelgas, J., Wikström, H., Hsiao, W.K., Folestad, S., Korhonen, O., Abrahmsén-Alami, S., Tajarobi, P., 2020. Robustness of a continuous direct compression line against disturbances in feeding. Int. J. Pharm. 574, 118882 https://doi.org/10.1016/j.ijpharm.2019.118882.

Kerins, B.M., Crean, A.M., 2022. Continuous Powder Feeding: Equipment Design and Material Considerations. Springer International Publishing, Cham, pp. 171–191. https://doi.org/10.1007/978-3-030-90924-6_7.

Kirchengast, M., Celikovic, S., Rehrl, J., Sacher, S., Kruisz, J., Khinast, J., Horn, M., 2019. Ensuring tablet quality via model-based control of a continuous direct compaction process. Int. J. Pharm. 567, 118457 https://doi.org/10.1016/j.ijpharm.2019.118457.

Lee, S.L., O'Connor, T.F., Yang, X., Cruz, C.N., Chatterjee, S., Madurawe, R.D., Moore, C. M.V., Yu, L.X., Woodcock, J., 2015. Modernizing pharmaceutical manufacturing: from batch to continuous production. J. Pharm. Innov. 10, 191–199. https://doi.org/10.1007/s12247-015-9215-8.

Oka, S.S., Sebastian Escotet-Espinoza, M., Singh, R., Scicolone, J.V., Hausner, D.B., Ierapetritou, M., Muzzio, F.J., 2017. Design of an Integrated Continuous Manufacturing System, pp. 405–446. https://doi.org/10.1002/9781119001348.ch12.

Pordesimo, L., Onwulata, C., Carvalho, C., 2009. Food powder delivery through a feeder system: effect of physicochemical properties. Int. J. Food Prop. 12, 556–570. https://doi.org/10.1080/10942910801947748.

Rasmussen, C.E., Williams, C.K.I., 2005. Gaussian Processes for Machine Learning. MIT Press.

Santos, B., Carmo, F., Schlindwein, W., Muirhead, G., Rodrigues, C., Cabral, L., Westrup, J., Pitt, K., 2018. Pharmaceutical excipients properties and screw feeder performance in continuous processing lines: a quality by design (QbD) approach. Drug Dev. Ind. Pharm. 44, 2089–2097. https://doi.org/10.1080/03639045.2018.1513024.

Shier, A.P., Kumar, A., Mercer, A., Majeed, N., Doshi, P., Blackwood, D.O., Verrier, H.M., 2022. Development of a predictive model for gravimetric powder feeding from an API-rich materials properties library. Int. J. Pharm. 625, 122071 https://doi.org/10.1016/j.ijpharm.2022.122071.

Singh, R., Ierapetritou, M., Ramachandran, R., 2013. System-wide hybrid MPC–PID control of a continuous pharmaceutical tablet manufacturing process via direct compaction. Eur. J. Pharm. Biopharm. 85, 1164–1182. https://doi.org/10.1016/j.ejpb.2013.02.019.

Stauffer, F., Vanhoorne, V., Pilcer, G., Chavez, P.F., Schubert, M., Vervaet, C., De Beer, T., 2019. Managing active pharmaceutical ingredient raw material variability during twin-screw blend feeding. Eur. J. Pharm. Biopharm. 135, 49–60. https://doi.org/10.1016/j.ejpb.2018.12.012.

Suzuki, Y., Sugiyama, H., Kano, M., Shimono, R., Shimada, G., Furukawa, R., Mano, E., Motoyama, K., Koide, T., Matsui, Y., Kurasaki, K., Takayama, I., Hikage, S., Katori, N., Kikuchi, M., Sakai, H., Matsuda, Y., 2021. Control strategy and methods for continuous direct compression processes. Asian J. Pharm. Sci. 16, 253–262. https://doi.org/10.1016/j.ajps.2020.11.005.

Tahir, F., Palmer, J., Khoo, J., Holman, J., Yadav, I.K., Reynolds, G., Meehan, E., Mitchell, A., Bajwa, G., 2020. Development of feed factor prediction models for loss-in-weight powder feeders. Powder Technol. 364, 1025–1038. https://doi.org/10.1016/j.powtec.2019.09.071.

Tian, G., Koolivand, A., Arden, N.S., Lee, S., O'Connor, T.F., 2019. Quality risk assessment and mitigation of pharmaceutical continuous manufacturing using flowsheet modeling approach. Comput. Chem. Eng. 129, 106508 https://doi.org/10.1016/j.compchemeng.2019.06.033.

Van Snick, B., Kumar, A., Verstraeten, M., Pandelaere, K., Dhondt, J., Di Pretoro, G., De Beer, T., Vervaet, C., Vanhoorne, V., 2019. Impact of material properties and process variables on the residence time distribution in twin screw feeding equipment. Int. J. Pharm. 556, 200–216. https://doi.org/10.1016/j.ijpharm.2018.11.076.

Waeytens, R., De Souter, L., Grymonpré, W., Van Hauwermeiren, D., Nopens, I., De Beer, T., 2022. An extended 3-compartment model for describing step change experiments in pharmaceutical twin-screw feeders at different refill regimes. Int. J. Pharm. 627, 122154 https://doi.org/10.1016/j.ijpharm.2022.122154.

Wang, Y., Li, T., Muzzio, F.J., Glasser, B.J., 2017a. Predicting feeder performance based on material flow properties. Powder Technol. 308, 135–148. https://doi.org/10.1016/j.powtec.2016.12.010.

Wang, Z., Escotet-Espinoza, M.S., Ierapetritou, M., 2017b. Process analysis and optimization of continuous pharmaceutical manufacturing using flowsheet models. Comput. Chem. Eng. 107, 77–91. https://doi.org/10.1016/j.compchemeng.2017.02.030.

Wang, Y., O'Connor, T., Li, T., Ashraf, M., Cruz, C.N., 2019. Development and applications of a material library for pharmaceutical continuous manufacturing of solid dosage forms. Int. J. Pharm. 569, 118551 https://doi.org/10.1016/j.ijpharm.2019.118551.

Yadav, I.K., Holman, J., Meehan, E., Tahir, F., Khoo, J., Taylor, J., Benedetti, A., Aderinto, O., Bajwa, G., 2019. Influence of material properties and equipment configuration on loss-in-weight feeder performance for drug product continuous manufacture. Powder Technol. 348, 126–137. https://doi.org/10.1016/j.powtec.2019.01.071.